MCB
Journals.ASM.org

Lack of tRNA Modification Isopentenyl-A37 Alters mRNA Decoding and Causes Metabolic Deficiencies in Fission Yeast

Tek N. Lamichhane,[a] Nathan H. Blewett,[a]* Amanda K. Crawford,[a]* Vera A. Cherkasova,[a] James R. Iben,[a] Thomas J. Begley,[b] Philip J. Farabaugh,[c] Richard J. Maraia[a,d]

Intramural Research Program, NICHD, NIH, Bethesda, Maryland, USA[a]; College of Nanoscale Science and Engineering, University at Albany, Albany, New York, USA[b]; Department of Biological Sciences, University of Maryland Baltimore County, Baltimore, Maryland, USA[c]; Commissioned Corps, U.S. Public Health Service, Washington, DC, USA[d]

tRNA isopentenyltransferases (Tit1) modify tRNA position 37, adjacent to the anticodon, to N^6-isopentenyladenosine (i6A37) in all cells, yet the tRNA subsets selected for modification vary among species, and their relevance to phenotypes is unknown. We examined the function of i6A37 in *Schizosaccharomyces pombe tit1*$^+$ and *tit1*-Δ cells by using a β-galactosidase codon-swap reporter whose catalytic activity is sensitive to accurate decoding of codon 503. i6A37 increased the activity of tRNA^{Cys} at a cognate codon and that of tRNA^{Tyr} at a near-cognate codon, suggesting that i6A37 promotes decoding activity generally and increases fidelity at cognate codons while decreasing fidelity at noncognate codons. *S. pombe* cells lacking *tit1*$^+$ exhibit slow growth in glycerol or rapamycin. While existing data link wobble base U34 modifications to translation of functionally related mRNAs, whether this might extend to the anticodon-adjacent position 37 was unknown. Indeed, we found a biased presence of i6A37-cognate codons in high-abundance mRNAs for ribosome subunits and energy metabolism, congruent with the observed phenotypes and the idea that i6A37 promotes translational efficiency. Polysome profiles confirmed the decreased translational efficiency of mRNAs in *tit1*-Δ cells. Because subsets of i6A37-tRNAs differ among species, as do their cognate codon-sensitive mRNAs, these genomic variables may underlie associated phenotypic differences.

tRNAs contain nucleotide modifications, residing mostly in the tRNA body, that confer a range of activities (reviewed in references 1 and 2). Another class of modifications occurs in the anticodon loop (ACL), mostly at positions 34 and 37, and contributes to tRNA fit in the ribosome decoding center and to codon-anticodon interactions (3–5). Positions 34 and 37 bear the most diverse modifications, with some requiring multiple enzymatic activities (1). Position 34 modifications control the ability of tRNA to wobble to synonymous codons and/or restrict pairing with noncognate codons (5). The TRM9 U34 methyltransferase modification occurs on a subset of tRNAs that sensitize specific mRNAs bearing a high abundance of cognate codons that contribute to a DNA damage response (6). A different U34 modification on different tRNAs sensitizes other mRNAs with cognate codon usage (7).

Position 37 is considered part of the extended anticodon (8) and can carry three types of modification: N^6-isopentenyladenosine (i6A), N^6-threonylcarbamoyladenosine (t6A) or its cyclized derivative ct6A (in bacteria and archaea) (9), and wybutosine (yW), among which the A37 variety is further modified in some organisms. In bacteria, i6A37 is modified to 2-methylthio-N^6-isopentenyladenosine-37 (ms2i6A37) and/or the hydroxyl derivative, ms2i(o)6A37, whereas in eukaryotes it remains i6A37. The i6A37 and (c)t6A37 modifications occur on nonoverlapping sets of tRNAs and function to strengthen the adjacent (position 36), weak anticodon-codon pairs A-U and U-A, respectively, in the ribosome decoding center (5). It was recently reported that Cdkal1, encoded by a risk gene for type 2 diabetes (10), methylthiolates t6A37 to ms2t6A37 on tRNA^{Lys}UUU, and its deletion leads to type 2 diabetes in mice (11).

Translational misreading can have positive or negative effects on growth (reviewed in reference 12). Misreading is largely affected by competition among tRNAs for ribosome fit and codon match, and depending on the system at hand, rates can vary from 10^{-3} to 10^{-5} (13–15). A potential source of differing rates might be the species-specific composition of the tRNA gene complement (tRNAome) (16). Consistent with this possibility are mutants in Maf1, a repressor of tRNA synthesis, that exhibit asymmetric increases in the levels of different tRNAs and increased translational fidelity at UAA and UAG codons (17).

The MiaA gene encodes the *Escherichia coli* i6A-transferase, and its eukaryotic homologs encode Tit1 in *Schizosaccharomyces pombe*, MOD5 in *Saccharomyces cerevisiae*, the life span gene product GRO-1 in *Caenorhabditis elegans*, and the tumor suppressor TRIT1 in humans (18–23). Curiously, i6A37 occurs on different subsets of tRNAs in different model organisms. In bacteria, ms2i6A37 or ms2i(o)6A37 is found on tRNAs for UNN codons, i.e., for Cys, Leu, Phe, Ser, Trp, and Tyr (2, 24). In eukaryotes, i6A37 is significantly more restricted, as it is found on tRNAs for Ser, Tyr, and sometimes Cys or Trp. tRNA^{Cys}GCA carries i6A37 in *S. cerevisiae* but not in *S. pombe*, whereas tRNA^{Trp}CCA carries

Received 8 March 2013 **Returned for modification** 11 April 2013
Accepted 17 May 2013
Published ahead of print 28 May 2013
Address correspondence to Richard J. Maraia, maraiar@mail.nih.gov.
* Present address: Nathan H. Blewett, Program in Biomedical Sciences, University of Michigan, Ann Arbor, Michigan, USA; Amanda K. Crawford, College of Medicine, Howard University, Washington, DC, USA.
R.J.M. dedicates this work to the memory of Pierre Thuriaux.
Supplemental material for this article may be found at http://dx.doi.org/10.1128/MCB.00278-13.

doi:10.1128/MCB.00278-13

TABLE 1 Strains used in this study

Strain	Genotype	Reference or source
yYH1	*h*$^-$ *leu1-32*::[*tRNAmSer7T-leu1*$^+$] *ura4-D18 ade6-704*	71
yNB5	*h*$^-$ *leu1-32*::[*tRNAmSer7T-leu1*$^+$] *ura4-D18 tit1*-Δ::*KanMX6*$^+$ *ade6-704*	18
yAS99	*h*$^-$ *leu1-32 ura4-D18 ade6-704*	72
yTL1	*h*$^-$ *leu1-32 ura4-D18 ade6-704 tit1*-Δ::*KanMX6*	This report

i6A37 in *S. pombe* but not in *S. cerevisiae* (18), and the distribution in humans differs from those in both yeasts (T. N. Lamichhane and R. J. Maraia, unpublished data).

i6A37 does not affect charging, as yeast tRNAs lacking or containing i6A37 are equally aminoacylated (25), consistent with work on *E. coli* showing that the modification increases the efficiency of ribosome binding but not aminoacylation (reviewed in references 24 and 26). A lack of i6A37 derivatives slows bacterial cell growth (27–29). In the yeasts *S. cerevisiae* and *S. pombe*, the defects known to be attributable to a lack of i6A37 are due to decreased activity of mutant tRNAs known as suppressors (18, 19, 25, 30, 31). Suppressor tRNA activity reflects competition with translation termination/release factors, whereas natural tRNAs compete only with each other during normal elongation. In yeast, the absence of i6A37 decreases suppressor tRNA-mediated suppression but has little effect on growth (19, 25, 30).

A crystal structure of the bacterial ribosome-mRNA-tRNA^{Phe} complex shows that the sulfur moiety of ms2i6A37-tRNA^{Phe} makes direct contacts with and stabilizes the codon-anticodon interaction (32). Yet, as noted above, sulfonation of i6A37 does not occur in eukaryotes. To our knowledge, the function of tRNA-i6A37 in normal translation has not been examined in any eukaryotic system. Moreover, while published data link modifications of the wobble base U34 to translation of mRNA subsets related to observable phenotypes, whether or not this would be extendable to the anticodon-adjacent position 37 was unknown.

We provide evidence that i6A37 increases the functional efficiency of tRNAs to which it is added for cognate and near-cognate codons in *S. pombe*, increasing fidelity at cognate codons while decreasing fidelity at noncognate codons. Depletion of i6A37 by Tit1 deletion appears to reset levels of tRNA competition and misreading, translational efficiency, and translational fidelity. The data indicate that there is a translational deficiency in *tit1*-Δ cells that leads to rapamycin sensitivity and slow growth in glycerol. Computational searches for biased use of synonymous cognate codons for i6A37-tRNAs identified highly abundant mRNAs for ribosome subunits, translation factors, and enzymes involved in energy metabolism, congruent with observed phenotypes. Because subsets of i6A37-containing tRNAs vary among species, as do mRNAs with cognate codon biases, these genome-specific parameters may help to explain the diverse phenotypes associated with i6A37.

MATERIALS AND METHODS

S. pombe strains used in this study are listed in Table 1. *S. pombe* cells were seeded to an optical density at 600 nm (OD_{600}) of 0.1 and grown until an OD_{600} of 0.5, and 10-fold dilutions were plated on appropriate medium. For rapamycin (AG Scientific Inc.) treatment, cells were treated with the indicated concentrations for 2 h or with the drug vehicle (dimethyl sulfoxide [DMSO]; Sigma). For mitochondrial tRNA (mt-tRNA) analysis, cells were grown in Edinburgh minimal medium (EMM) lacking uracil.

Plasmids. *lacZ* was amplified from *E. coli* and cloned into pREP4X with a 3×-FLAG tag at the C terminus. The UAC sequence at codon 503 was changed to UGC by site-directed mutagenesis. tRNA^{Cys}-G37 from *S. pombe*, including 200 bp upstream, was amplified, cloned into pREP3X, and then subjected to site-directed mutagenesis to create tRNA^{Cys}-A37. All constructs were confirmed by sequencing.

RNA preparation and Northern blotting. Cells were grown to an OD_{600} of 0.5 in appropriate medium. Purified RNA was electrophoresed in Novex 10% Tris-borate-EDTA (TBE)–urea gels, transferred to GeneScreen nylon by use of an Invitrogen iBlot device, and probed with ^{32}P-labeled oligonucleotides as described previously (18).

Protein extraction and Western blotting. Cells were grown to an OD_{600} of 0.5, and protein was extracted in lysis buffer (150 mM NaCl, 50 mM Tris-Cl, pH 7.5, 1 mM EDTA, 0.1% NP-40, and 0.1 mM phenylmethylsulfonyl fluoride [PMSF]), using glass beads and a Biospec Mini-Beadbeater 4 times for 30 s each, with 1 min on ice between beatings. Debris was pelleted, and the supernatant was collected, quantified by the Bradford assay, analyzed by 4 to 12% Bis-Tris PAGE (Novex), stained with Ponceau S, rinsed, and transferred to nitrocellulose by use of an Invitrogen iBlot transfer apparatus.

Beta-galactosidase. *tit1*$^+$ and *tit1*-Δ cells were grown to an OD_{600} of 0.5 and resuspended in 100 mM Tris-HCl, pH 8, 1 mM dithiothreitol (DTT), and 20% glycerol. Total protein was prepared and quantified by the Bio-Rad Bradford assay. Equal amounts of protein were used. *ortho*-Nitrophenyl-β-galactoside (ONPG) was freshly prepared in Z buffer (60 mM $Na_2HPO_4 \cdot 7H_2O$, 40 mM $NaH_2PO_4 \cdot H_2O$, 10 mM KCl, 1 mM $MgSO_4$, 5 mM β-mercaptoethanol, pH 7.0). A solution of 1 mg ONPG was incubated with protein at 37°C. With wild-type *lacZ*, 100 μg protein was incubated for 10 min; with *lacZ* encoding a protein with the Y503C mutation (*lacZ*-Y503C), 1 mg protein was incubated for 16 h. Reactions were stopped with 1 mM sodium carbonate. Absorbance was measured at 420 nm, and *lacZ* activity was calculated as described previously (Stratagene) (33).

Polysome profiles were obtained from fresh extracts made from yYH1 and yNB5 cells after growth in yeast extract with supplements (YES) medium, using a programmable density gradient fractionation system spectrophotometer (Foxy Jr.; Teledyne Isco, Lincoln, NE) with a gradient master (Biocomp) as described previously (34). Specific mRNAs were analyzed by Northern blotting.

[^{35}S]methionine labeling. Wild-type and *tit1*-Δ strains were grown in 5 ml EMM in the presence of DMSO or rapamycin (100 ng/ml). After the OD_{600} reached 0.5, 150 μCi of [^{35}S]methionine (PerkinElmer) was added, and the cells were pulse labeled for 30 min at 32°C. Equal volumes of ice-cold water were added to each culture, and the cells were harvested. The cells were resuspended in 1 ml ice-cold water. Washed cells were harvested and whole-cell extracts separated by 10% PAGE. Gels were stained with SimplyBlue (Invitrogen, Carlsbad, CA), fixed, dried, and quantified with VisionWorks software to confirm that signals were in the linear range. Quantification of ^{35}S was performed with a model FLA3000 phosphorimager. The ratios of ^{35}S to SimplyBlue stain for 3 independent experiments were averaged and plotted.

Generation of codon-biased gene lists and GO term enrichment. Based on previously developed methods (6), codon bias was defined utilizing a simple metric of the number of i6A37-tRNA cognate codons versus the total number of synonymous codons. UCU codon or i6A37-tRNA(Ser) cognate codon counts versus total serine codon counts were compiled over all *S. pombe* mRNAs (GenBank accession no. GCF_000002945.1). Based upon fractional compositions, a *Z* score was derived for each gene as a metric of individual gene codon bias. Lists were generated based upon gene *Z*-score sorting. From each list, the top 200 genes were selected and subjected to gene ontology (GO) term enrichment analysis by AmiGO (35).

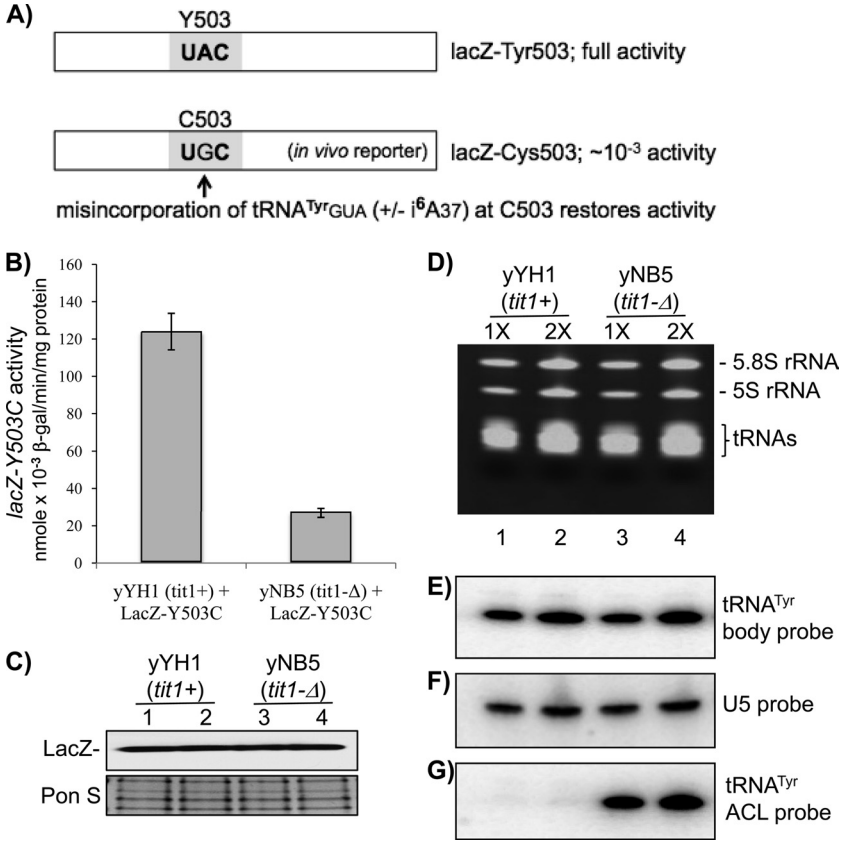

FIG 1 i6A37 increases competitive decoding activity of tRNA^{Tyr}GUA at a near-cognate codon. (A) Schematic of experimental design. (B) *lacZ* activities of extracts from yYH1 (*tit1*$^+$) and yNB5 (*tit1*-Δ) cells after transformation with *lacZ*-Y503C. Error bars reflect the ranges for triplicate experiments. (C) Immunoblot detection of FLAG-tagged LacZ-Y503C protein in extracts used for panel B, using anti-FLAG antibody (upper panel). (Lower panel) Ponceau S (Pon S)-stained gel prior to transfer, as a loading control. (D to G) RNA analysis. (D) Ethidium bromide-stained denaturing polyacrylamide gel used to make a blot that was sequentially probed as indicated to the right of panels E to G (see the text). Total RNAs from yYH1 (*tit1*$^+$) and yNB5 (*tit1*-Δ) cells were loaded at two concentrations, i.e., 1× (5 μg) and 2× (10 μg), as indicated above the lanes.

Nomenclature note. The *S. pombe* gene that encodes the tRNA isopentenyltransferase was initially named *sin1* (30, 31), but subsequently, another gene was officially named *sin1* in the contemporary *S. pombe* database. Therefore, we had to choose another name.

RESULTS

i6A37 increases translation-decoding activity of tRNA^{Tyr}GUA. ACL modifications decrease tRNA rejection by the translating ribosome (36). An *in vivo* reporter that monitors amino acid misincorporation based on a mutant firefly luciferase with inactivating mutations in the essential active site residue lysine-529 has been used to monitor decoding of specific codons in yeast and bacteria (13, 15). However, lysine is not among the tRNAs that carry i6A37 in *S. pombe*, which are three tRNA^{Ser} species (DGA; D = A, C, or U) that decode four of the six Ser codons; tRNA^{Tyr}GUA, which decodes both Tyr codons; and tRNA^{Trp}CCA, which decodes the Trp codon (18). A reporter that is applicable for our purpose is β-galactosidase (*lacZ*), which requires Tyr at position 503 for enzymatic activity (37, 38). While activity was severely diminished by amino acid substitutions at this position, the resulting LacZ proteins suffered no detectable change in overall structure or stability (37–39). Tyr-503 is encoded by UAC and decoded in *S. pombe* by tRNA^{Tyr}GUA containing i6A37 (18). We cloned *lacZ* into an *S. pombe* expression vector and mutated the second position (A) of the Tyr-503 UAC codon to G to create the near-cognate Cys codon UGC; the resultant gene is referred to as *lacZ*-Y503C. Thus, only if tRNA^{Tyr}GUA misread the UGC 503 codon would *lacZ*-Y503C activity be observed. Consistent with expected misreading rates, we observed an ~1,000-fold decrease in *lacZ* activity due to replacement of the Tyr-503 codon with the UGC Cys codon in *S. pombe* (not shown) (Fig. 1A). For the present study, we used *lacZ*-Y503C as an *in vivo* reporter.

We first used *lacZ*-Y503C to compare activities in the wild-type *tit1*$^+$ (yYH1) and *tit1*-Δ (yNB5) strains, in which tRNA^{Tyr}GUA is modified with i6A37 and unmodified, respectively (18). *S. pombe* tRNA^{Cys}GCA has an encoded G at position 37 and is not a Tit1 substrate in either strain (18), so it was not a variable here. We observed higher *lacZ* activity in *tit1*$^+$ cells than in *tit1*-Δ cells (Fig. 1B). There was no difference in the amounts of LacZ protein accumulated in these cells as monitored by anti-FLAG immunoblotting (duplicate loadings) (Fig. 1C). Thus, i6A37 on tRNA^{Tyr}GUA caused misreading of the near-cognate Cys codon. We showed previously that i6A37 does not affect levels of tRNA^{Ser} or tRNA^{Trp} in *S. pombe* (18). We showed this here for tRNA^{Tyr} in the cells used for *lacZ* analysis: there was no significant difference in *tit1*$^+$ and *tit1*-Δ cells (Fig. 1D to F). Differential i6A37 modification of tRNA^{Tyr}GUA in the *tit1*$^+$ and *tit1*-Δ cells was confirmed using the

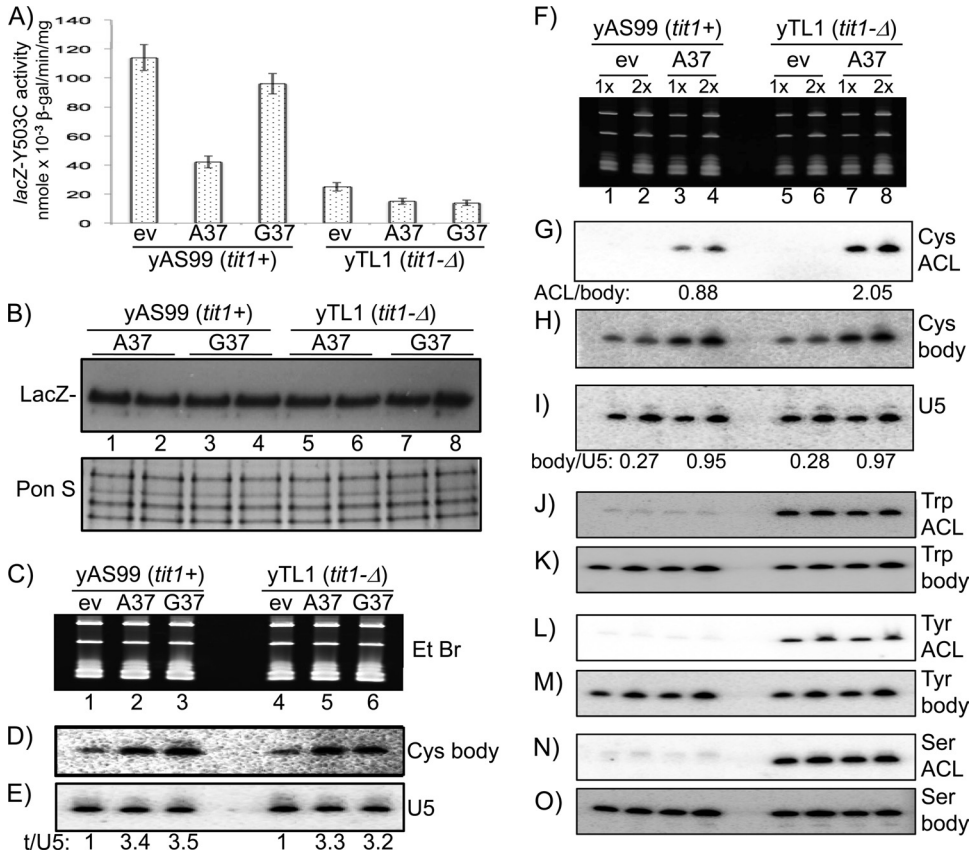

FIG 2 i6A37 increases tRNA^{Cys}GCA activity at its cognate codon. (A) *lacZ*-Y503C activities as shown in Fig. 1, after transformation of yYH1 (*tit1*$^+$) and yTL1 (*tit1*-Δ) cells with empty vector (ev) or vector containing the *S. pombe* tRNA^{Cys}GCA-G37 or tRNA^{Cys}GCA-A37 gene, as indicated below the bars. (B) Immunoblot detection of FLAG-tagged LacZ-Y503C protein in extracts used for panel A, using anti-FLAG antibody (upper panel). (Lower panel) Ponceau S-stained gel prior to transfer, as a loading control. (C to E) Analysis of tRNA^{Cys}GCA-G37 and tRNA^{Cys}GCA-A37 levels. (C) Ethidium bromide (EtBr)-stained gel used to make a blot that was sequentially probed as indicated to the right of panels D and E for comparison of expression of ectopic tRNA^{Cys}GCA-G37 and tRNA^{Cys}GCA-A37 by use of a body probe that has perfect complementarity to both, with U5 RNA as a loading control. Quantitation of U5 and tRNA levels was done by phosphorimager analysis, and the relative ratios are indicated below the lanes. (F to I) Analysis of i6A37 modification of tRNA^{Cys}GCA-A37. (F) Ethidium bromide-stained gel. (G) Blot probed for i6A37 modification of tRNA^{Cys}GCA-A37 by use of the PHA6 assay. See the text for interpretation of the quantification shown under the lanes. (H) Blot probed for tRNA^{Cys}GCA-G37 and tRNA^{Cys}GCA-A37 by use of a body probe with perfect complementarity to both. (I) Blot probed for U5 snRNA. Quantitation of U5 and tRNA levels in panels H and I was done by phosphorimager analysis, and the relative ratios are indicated below the lanes. (J to O) ACL and body probing for tRNA^{Trp}, tRNA^{Tyr}, and tRNA^{Ser}AGA on the same blot, as indicated to the right of the panels.

PHA6 assay (positive hybridization in the absence of i6A37), in which the signal intensity increases as modification decreases (18) (Fig. 1G). The i6A modification decreases hybridization with an oligonucleotide probe because the large, bulky, hydrophobic isopentenyl group on N^6 of A interferes with base pairing to T. The data suggest that i6A37-tRNA^{Tyr}GUA competes ~4 times better than unmodified tRNA^{Tyr}GUA for the near-cognate *lacZ* UGC 503 codon.

This result was counterintuitive to the expectation that the presence of a modification should improve rather than worsen decoding fidelity. The presence of mnm5s2 on wobble base U34 of tRNA^{Lys} was unexpectedly found to increase third-position codon misreading in bacteria (40). To our knowledge, increased second-position misreading due to the presence of i6A37 had not previously been observed.

The unexpected results with tRNA^{Tyr}GUA raised the question of how i6A37 would affect the decoding fidelity of a tRNA for its cognate codon. To answer this question, we monitored the degree to which tRNA^{Cys}GCA in the i6A37-modified versus unmodified state could prevent decoding by tRNA^{Tyr}GUA by using *lacZ*-Y503C. While tRNA^{Cys}GCA from bacteria and eukaryotes, including the yeast *S. cerevisiae*, contains i6A37, the *S. pombe* tRNA-^{Cys}GCA does not, because its tRNA^{Cys}GCA genes encode G rather than A at position 37 (18, 41; http://gtrnadb.ucsc.edu/). We could circumvent this with an *S. pombe* tRNA^{Cys}GCA gene whose position 37 was changed from G to A by single nucleotide mutagenesis, comparing the tRNA^{Cys}GCA-G37 and tRNA^{Cys}GCA-A37 genes for *lacZ*-Y503C activity in the *tit1*$^+$ and *tit1*-Δ strains.

i6A37 increases tRNA^{Cys}GCA activity at its cognate codon. We cloned the *S. pombe* tRNA^{Cys}GCA gene into a plasmid. Point mutation of tRNA^{Cys}GCA G37 to A37 created an A36A37A38 recognition site for Tit1p (18). For plasmid selection, we needed to use another *tit1*-Δ strain, yTL1, and its *tit1*$^+$ isogenic control, yAS99 (Fig. 2).

According to tRNA competition, an increase in tRNA^{Cys}GCA levels would decrease the *lacZ*-Y503C activity resulting from misreading by tRNA^{Tyr}GUA-i6A37 in *tit1*$^+$ cells. While tRNA^{Cys}-GCA-G37 and -A37 decreased *lacZ*-Y503C activity, the A37 resi-

due did so more than the G37 residue in the *tit1*$^+$ strain (Fig. 2A). Significantly, in contrast to the case with the *tit1*$^+$ strain, tRNA^{Cys}GCA-G37 and -A37 decreased activity to the same extent in *tit1*-Δ cells, in which neither tRNA contains i6A37 (Fig. 2A and B).

We examined the tRNAs and found similar expression from the ectopic tRNA^{Cys}GCA-A37 and -G37 genes with a probe complementary to their identical ψ stem-loops (Fig. 2C and D, "body" probe). Normalization to U5 RNA revealed that tRNA^{Cys}GCA in the transformed cells accumulated to about 3-fold higher levels than those of endogenous tRNA^{Cys}GCA (Fig. 2E).

We next examined the i6A37 modification status of ectopic tRNA^{Cys}GCA-A37 in the *tit1*$^+$ cells by using the PHA6 assay. The ACL A37 probe detected ectopic tRNA^{Cys}GCA-A37 without cross-reactivity with endogenous tRNA^{Cys}GCA-G37 (Fig. 2F and G). A detectable signal from *tit1*$^+$ cells (Fig. 2G, lanes 3 and 4) indicated that the extent of i6A37 modification of ectopic tRNA^{Cys}GCA-A37 was incomplete, consistent with partial modification due to overexpression. Quantification after normalization to the body probe (Fig. 2H) indicated that tRNA^{Cys}GCA-A37 was modified only ~57% in the *tit1*$^+$ cells (Fig. 2G) {the ACL/body ratio was calculated as follows: $[1 - (0.88/2.05)] \times 100$}. Accounting for incomplete modification suggests that i6A37 increased the specific activity of tRNA^{Cys}GCA-A37 for its cognate codon almost 4-fold relative to that of unmodified tRNA^{Cys}GCA. Quantification using U5 snRNA showed similar loading and relative expression levels of the ectopic tRNAs (Fig. 2I). Analysis of endogenous tRNA^{Trp}, tRNA^{Tyr}, and tRNA^{Ser}AGA on the same blot showed full modification (Fig. 2J to O), suggesting that the hypomodification in these strains was limited to the ectopic tRNA^{Cys}GCA-A37.

In summary, the data for *tit1*$^+$ cells indicate that tRNA^{Cys}GCA-i6A37 competes better than tRNA^{Cys}GCA-G37 for the cognate codon. The data for *tit1*-Δ cells argue that unmodified tRNA^{Cys}-GCA-A37 and -G37 compete equally against unmodified tRNA^{Tyr}GUA. tRNA^{Cys}GCA-G37 decreased *lacZ*-Y503C activity by 15% and 40% in the *tit1*$^+$ and *tit1*-Δ strains, respectively, which is reflective of the differential competition by modified and unmodified tRNA^{Tyr}GUA in the two strains. A conclusion is that the absence of i6A37 due to *tit1* deletion disrupts the homeostasis of codon misreading in *S. pombe*.

Deletion of *tit1*$^+$ causes sensitivity to rapamycin. Increases in mistranslation can lead to positive or negative effects on growth (reviewed in references 12 and 42). Unlike growth of *S. cerevisiae* and human cells *in vitro*, normal growth of *S. pombe* is insensitive to rapamycin, a small-molecule drug that inhibits TOR kinases that control growth and proliferation in response to nitrogen, amino acids, and other nutrients (43, 44). Rapamycin does impose adverse effects on *S. pombe*, but they are not quite severe enough to slow growth, because its inhibition of the *tor2*$^+$ component of TORC1 is only partial (45). Defects in nuclear tRNA metabolism in *sla1*-Δ mutants lacking the pre-tRNA chaperone known as La protein lead to a nutritional stress response manifested by leucine uptake deficiency, increased expression of amino acid-metabolizing (AAM) genes, and sensitivities to NH_3 and rapamycin, indicative of TOR system perturbation (46).

While yYH1 (*tit1*$^+$) and yNB5 (*tit1*-Δ) grew similarly on EMM, yNB5 growth was inhibited by rapamycin (Fig. 3A). Slow growth in rapamycin was rescued by ectopic *tit1*$^+$ (yNB5 plus *tit1*$^+$) and *S. cerevisiae MOD5* but not by the previously characterized *tit1*-T12A catalytic mutant (18) (Fig. 3A).

We examined incorporation of [^{35}S]methionine into newly synthesized proteins. [^{35}S]methionine was added to cells in log-phase growth in the presence or absence of rapamycin. Thirty minutes after addition of [^{35}S]methionine, extracts were prepared, loaded in triplicate at 1×, 2×, and 4× concentrations, fractionated in SDS gels, stained with Coomassie blue, photographed (Fig. 3B), dried, and subjected to autoradiography (Fig. 3C). No significant differences in ^{35}S incorporation were evident in *tit1*$^+$ cells in the presence or absence of rapamycin or in *tit1*-Δ cells in its absence (Fig. 3B and C, lanes 1 to 9). *tit1*-Δ cells incorporated less ^{35}S in the presence of rapamycin than did the other cells (Fig. 3B and C, compare lanes 7 and 8 to lanes 10 and 11), consistent with their decreased growth rate. The reproducible qualitative differences described below were more significant observations.

Inspection of the gels revealed a differential pattern in the rapamycin-treated *tit1*-Δ cell extract relative to the other three samples. Two major bands were specifically decreased in the rapamycin-treated *tit1*-Δ cells relative to the untreated *tit1*-Δ cells and the *tit1*$^+$ cells, as apparent in the Coomassie gel and the autoradiograph (Fig. 3B and C, asterisks). This differential pattern is evidence of more than just a general reduction of protein synthesis and suggests a response to rapamycin that is specific to *tit1*-Δ cells. The identities of the relevant proteins are currently unknown and are beyond the scope of the present study.

We also observed a morphological response to rapamycin by *tit1*-Δ cells. While *tit1*-Δ and *tit1*$^+$ cells appeared to be similar in the absence of rapamycin, *tit1*-Δ cells were relatively shortened after exposure to rapamycin (Fig. 3D). *S. pombe* cell shortening is a characteristic of the *wee1* mutant phenotype and also occurs under certain stress conditions and in TOR mutants (47–49). The Wee1 kinase integrates signals that serve to coordinate cell size and cell cycle progression such that cells that have grown sufficiently in mass, reflective of adequate ribosome production, may undergo cell division and proliferation (50, 51). We measured the lengths of 50 cells in the presence of rapamycin and 50 cells in its absence for each of the strains/conditions represented by the panels in Fig. 3D and plotted their lengths relative to those of the no-rapamycin controls (Fig. 3E). While rapamycin reduced the length of *tit1*$^+$ (yYH1) cells by 10%, it caused a more significant reduction in *tit1*-Δ cell length that was largely reversed by ectopic *tit1*$^+$ (Fig. 3E).

***tit1*-Δ cells exhibit slow growth in glycerol.** Slow growth in media containing glycerol as the carbon source reflects mitochondrial deficiency (52). Mod5 is targeted to mitochondria and modifies mt-tRNAs (19, 53–55). It was not known if Tit1 is targeted to mitochondria, although multiple computational programs predicted that it would be (see Discussion). Because *mod5* mutants do not exhibit slow growth in glycerol (56; A. Hopper, OSU, personal communication), it is significant that yNB5 does (Fig. 4A). This defect was rescued by ectopic *tit1*$^+$ but not by the *tit1*-T12A catalytic mutant, and slightly less so by *MOD5* (Fig. 4A).

MiaA and Tit1 modify tRNAs with the sequence AAA at ACL positions 36 to 38 (18, 21, 57). Examination of all *S. pombe* mitochondrion-encoded tRNA sequences for this feature identified mt-tRNA^{Trp} as a potential Tit1 substrate. Analysis of *in vivo* modification of mt-tRNA^{Trp} by the PHA6 assay indeed suggested significant modification (Fig. 4B, C, and D). Probing of the same blot for mt-tRNA^{Cys} and mt-tRNA^{Ser}, neither of which was predicted to be a Tit1 substrate, revealed no significant difference between the ACL and body probes (Fig. 4E to H).

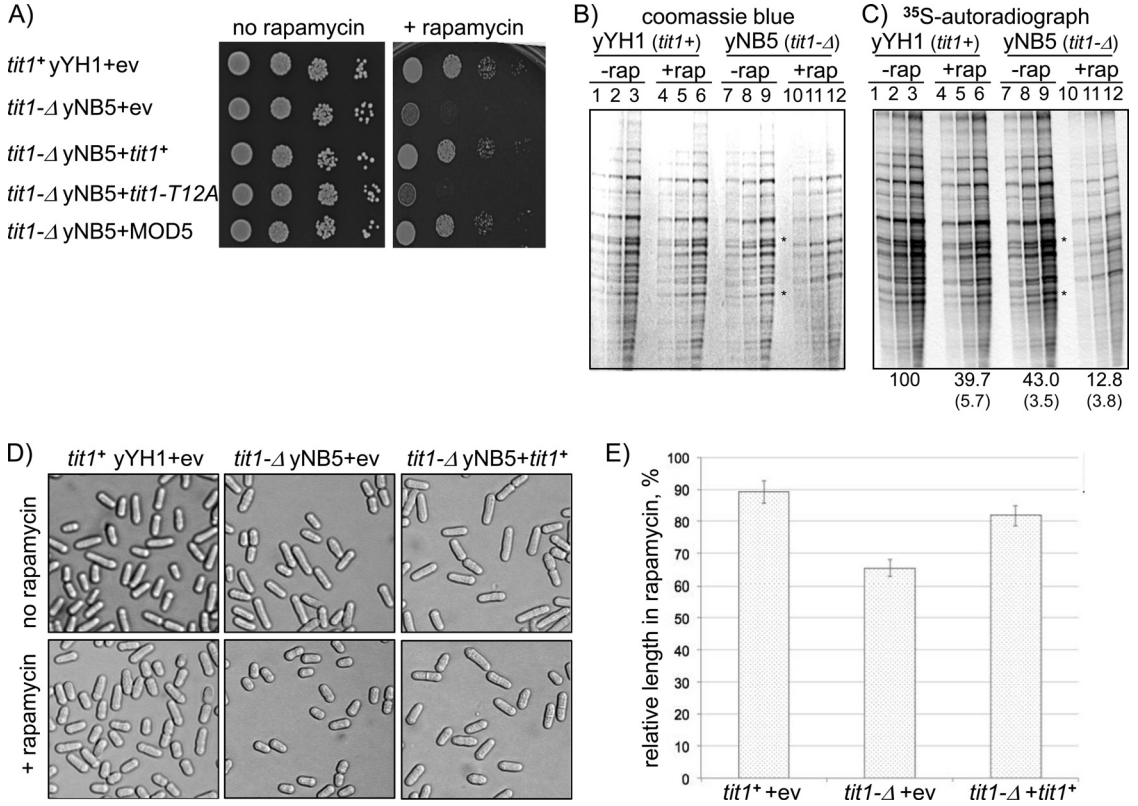

FIG 3 Deletion of *tit1*$^+$ causes growth and morphology phenotypes in rapamycin. (A) Comparative serial dilutions of *tit1*$^+$ and *tit1*-Δ cells in EMM lacking uracil (left panel; no rapamycin) or EMM lacking uracil but containing 50 μg/ml rapamycin (right panel; + rapamycin), after transformation with empty vector (+ev) or the indicated ectopic plasmid-borne genes: *S. pombe tit1*$^+$, the *tit1*-T12A catalytic mutant, and *S. cerevisiae MOD5* (see the text). (B) Coomassie blue-stained SDS gel of extracts after labeling with [^{35}S]methionine in the presence or absence of rapamycin (rap) as indicated above the lanes (each extract was loaded in triplicate, at 1×, 2×, and 4× concentrations). (C) The same gel as in panel B, but after drying and exposure to a phosphorimager to visualize ^{35}S-labeled proteins. The asterisks indicate bands specifically absent for rapamycin-treated *tit1*-Δ cells (see the text). Quantitation results from 3 independent experiments are reported under the lanes. Lanes from gels after Coomassie blue staining were quantified with VisionWorks software, which confirmed that the signals were in the linear range. ^{35}S was quantified with a FLA3000 phosphorimager. The ^{35}S/blue ratios relative to that of *tit1*$^+$ cells without rapamycin (100%) are reported. (D) Microscopic analysis of *tit1*$^+$ and *tit1*-Δ cells containing empty vector (+ev) or ectopic *tit1*$^+$, as indicated, in the absence (upper panels) or presence (lower panels) of rapamycin. (E) Quantitative analysis of cell length reduction by rapamycin for the three samples in panel D. Lengths of 50 cells from each of the samples represented by the six panels were measured. Cell length in the presence of rapamycin was expressed as % length in the absence of rapamycin. Error bars reflect standard deviations.

Quantitative data from five independent experiments provided statistically significant evidence that mt-tRNA^{Trp} is modified, albeit partially, in *tit1*$^+$ cells (Fig. 4I). Quantitative ACL and body probe data for the three mt-tRNA species examined were applied to the following formula: % modification = [1 − (ACL*tit1*$^+$/BP*tit1*$^+$)/(ACL*tit1*-Δ/BP*tit1*-Δ)] × 100, where "ACL" indicates the ACL probe and "BP" indicates the body probe. Note that this formula includes internal normalization by using the data from the *tit1*-Δ samples. The results suggest that although mt-tRNA^{Trp} was only partially modified in *tit1*$^+$ cells under the conditions examined, its hypomodification in *tit1*-Δ cells may have contributed to their glycerol-sensitive slow growth. When *tit1*$^+$ and *tit*-Δ cells were tested in YES (rich) medium or glycerol, the level of mt-tRNA^{Trp} modification was not significantly different from that for cells grown in EMM (not shown).

Identification of *S. pombe* mRNAs enriched in i6A37-tRNA cognate codons. Although codon use frequency is usually based on genomic averages, it can also be calculated for individual mRNAs relative to the genomic average (6). In *S. pombe*, three amino acids are delivered to the translating ribosome by i6A37-tRNAs: a subset of Ser tRNAs plus Tyr and Trp tRNAs (18). We took three computational approaches to identify mRNAs with a biased composition of i6A37-cognate codons whose translation might be affected by *tit1* deletion (6). We first examined the 5,006 *S. pombe* mRNAs for the most abundant Tit1 cognate codon, UCU (serine). tRNA^{Ser}AGA-i6A37 is encoded by 7 genes, a number equal to that of all other serine tRNA genes combined, and its cognate UCU codon is the most used serine codon in *S. pombe* (41; http://gtrnadb.ucsc.edu/). We examined the mRNAs for gene-specific overuse of UCU. For example, *rps1401* mRNA encodes the 40S ribosomal subunit protein S14, which is 140 amino acids long, and 4 of its 5 serine codons are UCU, representing an 80% use of UCU as the Ser codon, whereas the genomic average is 43%. This sorting identified ~200 mRNAs with overuse of UCU and enrichment *Z* scores of 1.7 to 5.8, most of which are abundant mRNAs for ribosomal proteins, translation factors, and enzymes involved in mitochondrion-based energy metabolism. We note that although mRNA abundance was not a criterion for sorting, it had been noted previously that abundant codons, including UCU, are found in abundant mRNAs in *S. cerevisiae* (58). Table 2 lists the

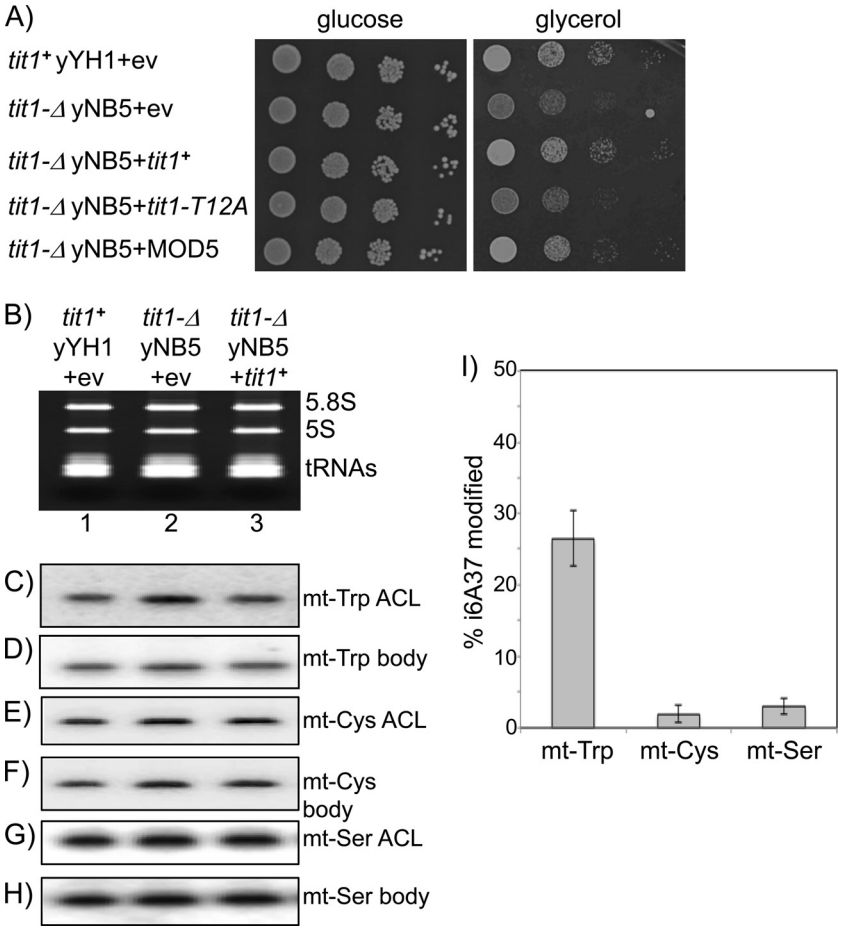

FIG 4 Deletion of *tit1*$^+$ causes i6A37 hypomodification of mt-tRNA^{Trp} and growth deficiency in glycerol. (A) Comparative serial dilutions of *tit1*$^+$ and *tit1*-Δ cells in EMM lacking uracil (left panel; glucose) or EMM lacking uracil but containing glycerol instead of glucose (right panel; glycerol), after transformation with empty vector (+ev) or the indicated ectopic plasmid-borne genes: *S. pombe tit1*$^+$, the *tit1*-T12A catalytic mutant, and *S. cerevisiae MOD5*. (B) Ethidium bromide-stained gel used to make a blot that was probed as shown in panels C to H. PHA6 Northern blot assays were used to compare the hybridization signals of ACL versus body probes for mitochondrial tRNAs mt-tRNA^{Trp}, mt-tRNA^{Cys}, and mt-tRNA^{Ser}, as indicated to the right of the panels. (I) Quantitative analysis of i6A37 modification of the 3 mt-tRNAs examined in panels B to H. Error bars reflect standard deviations for 5 experiments. Calculations for each mt-tRNA were performed as follows: % i6A37 modification = [1 − (ACL*tit1*$^+$/BP*tit1*$^+$)/(ACL*tit1*-Δ/BP*tit1*-Δ)] × 100. ACL, anticodon loop probe; BP, body probe.

top 30 mRNAs, and the full list of mRNAs is available in Dataset S1 in the supplemental material. Among the top 75 mRNAs are multiple mRNAs for mitochondrial proteins.

The output of this codon analysis was further analyzed using an *S. pombe* GO mapper. This revealed enrichments of the ribosomal subunit and of translation processes, with *P* values from 5.9×10^{-37} to 4×10^{-20}, as well as metabolic processes, with *P* values from 7.6×10^{-8} to 5.4×10^{-7} (Table 3).

The second approach was to identify mRNAs enriched in i6A37-cognate codons relative to synonymous codons decoded by tRNAs that do not contain i6A37. This would be only the four UCN Ser codons, because the other two Ser codons (AGY) are decoded by tRNA^{Ser}GCU, which is not modified by Tit1. All Tyr and Trp codons are decoded by i6A37-tRNAs, and synonymity is not an issue for these and therefore was not considered in this analysis. This identified ~200 mRNAs, with enrichment *Z* scores of 1.5 to 2.5, including mRNAs for ribosomal proteins, translation factors, and enzymes involved in energy metabolism (see Dataset S1 in the supplemental material) that largely overlapped the mRNAs identified by the first approach.

While the number of mRNAs identified by these approaches that consider bias with regard to synonymous codon use represent only ~5% of *S. pombe* genes, many of them, e.g., those encoding ribosomal proteins and translation factors, are expressed at high levels (see Dataset S1 in the supplemental material), suggesting the potential for significant impact.

The third approach was to identify mRNAs enriched in all i6A37-cognate codons relative to their overall genome averages for the four UCN Ser codons plus the two Tyr and one Trp codon, but without considering bias with regard to synonymous codon use. This identified 79 mRNAs, with enrichment *Z* scores of 2.08 to 7.78 (see Dataset S1 in the supplemental material), headed by the Wsc1 gene and followed by other genes related to the cell wall, including those encoding glycoproteins and enzymes involved in the major yeast cell wall component, 1,3-β-D-glucan. When these mRNAs were subjected to GO mapper analysis, the cell components identified were "cell surface" and "cell wall," with *P* values of 3.18×10^{-12} and 2.25×10^{-10}, respectively (see Dataset S1). Wsc1 is a cell wall-associated sensor of the cell wall integrity (CWI) pathway which communicates with TOR signaling (59).

TABLE 2 Top 30 mRNAs enriched in UCU codons

Locus	Gene name	Product	UCU *Z* score
SPBC19G7.03c	*rps3002*	40S ribosomal protein S30	5.830283744
SPBC211.05	*sab10*	Splicing factor 3B	5.830283744
SPAC3F10.18c	*rpl4102*	60S ribosomal protein L41	5.830283744
SPAC3G6.13c	*rpl4101*	60S ribosomal protein L41	5.830283744
SPBC29A3.07c	*sab14*	U2 snRNP-associated Sf3b14 homolog	5.830283744
SPAC11D3.01c	SPAC11D3.01c	Conserved fungal protein	5.830283744
SPCC1259.05c	*cox9*	Cytochrome *c* oxidase subunit VIIa	5.830283744
SPBC23G7.05	*sui1*	Translation initiation factor eIF1	5.830283744
SPBC25H2.07	*tif11*	Translation initiation factor eIF1A	5.830283744
SPAC1834.04	*hht1*	Histone H3 h3.1	4.590631652
SPAC664.04c	*rps1602*	40S ribosomal protein S16	4.590631652
SPAC13G6.07c	*rps601*	40S ribosomal protein S6	4.590631652
SPCC576.11	*rpl15*	60S ribosomal protein L15	4.495273799
SPAC25G10.06	*rps2801*	40S ribosomal protein S28	4.384022970
SPAC959.08	*rpl2102*	60S ribosomal protein L21	4.384022970
SPBC21B10.10	*rps402*	40S ribosomal protein S4	4.252544718
SPAP27G11.13c	*nop10*	snoRNP pseudouridylase H/ACA	4.094770815
SPAC3H5.05c	*rps1401*	40S ribosomal protein S14	4.094770815
SPAC1071.10c	*pma1*	P-type proton ATPase, P3-type Pma1	3.943856647
SPAC4A8.15c	*cdc3*	Profilin	3.901936045
SPBP8B7.06	*rpp201*	60S acidic ribosomal protein P2A	3.660892583
SPAC1705.02	SPAC1705.02	Human 4F5S homolog	3.660892583
SPAC22A12.04c	*rps2201*	40S ribosomal protein S15a	3.660892583
SPAC5D6.01	*rps2202*	40S ribosomal protein S15a	3.660892583
SPBC8D2.03c	*hhf2*	Histone H4 h4.2	3.660892583
SPBC1105.12	*hhf3*	Histone H4 h4.3	3.660892583
SPAC1834.03c	*hhf1*	Histone H4 h4.1	3.660892583
SPBC336.10c	*tif512*	Translation elongation factor eIF5A	3.660892583
SPCP1E11.09c	*rpp103*	60S acidic ribosomal protein Rpp1-3	3.660892583
SPAC644.15	*rpp101*	60S acidic ribosomal protein Rpp1-1	3.660892583

Finally, we examined the top-ranked (highest *Z* scores) 160 mRNAs in the three sets of computationally derived mRNAs for their abundances, using the mRNA copy number values of Marguerat et al. (60). This revealed that mRNAs with i6A37-sensitive codons that are overused relative to the synonymous i6A37-insensitive codons (i.e., the four i6A37-Ser UCN codons versus the other two Ser [AGY] codons) are highly skewed toward high abundance relative to all other mRNAs (see Dataset S1 in the supplemental material). The mRNAs identified by the third computational approach, i.e., those enriched in all i6A37 codons relative to their genomic averages but without considering bias with regard to synonymous codon use, more closely reflect the abundance distribution of most cellular mRNAs (see Dataset S1).

TABLE 3 GO analysis of top 200 mRNAs enriched in UCU codons

GO no.	GO term	*P* value
44391	Ribosomal subunit	5.92E−37
5840	Ribosome	3.67E−36
2181	Cytoplasmic translation	1.55E−27
6412	Translation	4.07E−20
44237	Cellular metabolic process	7.60E−08
8152	Metabolic process	4.04E−07
19538	Protein metabolic process	4.47E−07
44267	Cellular protein metabolic process	5.49E−07
10467	Gene expression	7.23E−07
42254	Ribosome biogenesis	1.77E−06
9987	Cellular process	3.22E−05
22613	RNP complex biogenesis	3.79E−05
44238	Primary metabolic process	2.11E−04
44249	Cellular biosynthetic process	4.52E−04
1901576	Organic substance biosynthetic process	4.61E−04
71704	Organic substance metabolic process	6.93E−04

Evidence of reduced translation efficiency in *tit1*-Δ cells. Polypeptide step time during translation elongation, codon context sensitivity, and translational efficiency were reduced in *Salmonella* and *E. coli* strains lacking i6A37 and derivatives due to mutation of MiaA (28, 61).

Analysis of polysome profiles has been used as an indicator of the efficiency of translation in yeast (62, 63). Lysates from yYH1 (*tit1*$^+$) and yNB5 (*tit1*-Δ) cells grown in parallel were subjected to sucrose gradient sedimentation for polysome analysis (Fig. 5A). Although the 60S and 80S peaks are merged in the gradients, accounting for their increased combined peak height, by superimposing the similarly sized 40S peaks, we observed a difference in polysome levels for *tit1*$^+$ and *tit1*-Δ cells, suggesting that *tit1*-Δ cells were compromised in translation (Fig. 5A). We quantified the ratios of 60S plus to 80S monosomes to polysomes for triplicate polysome profile experiments. As reported in the inset in Fig. 5A, the *tit1*-Δ cells had a significantly higher ratio than the *tit1*$^+$ cells, consistent with compromised translation in the *tit1*-Δ cells.

Polysome profiles can also be used to compare translation efficiencies of specific mRNAs. An mRNA that is efficiently translated is engaged by more ribosomes and resides on larger polyribosomes to a greater extent than when it is less efficiently

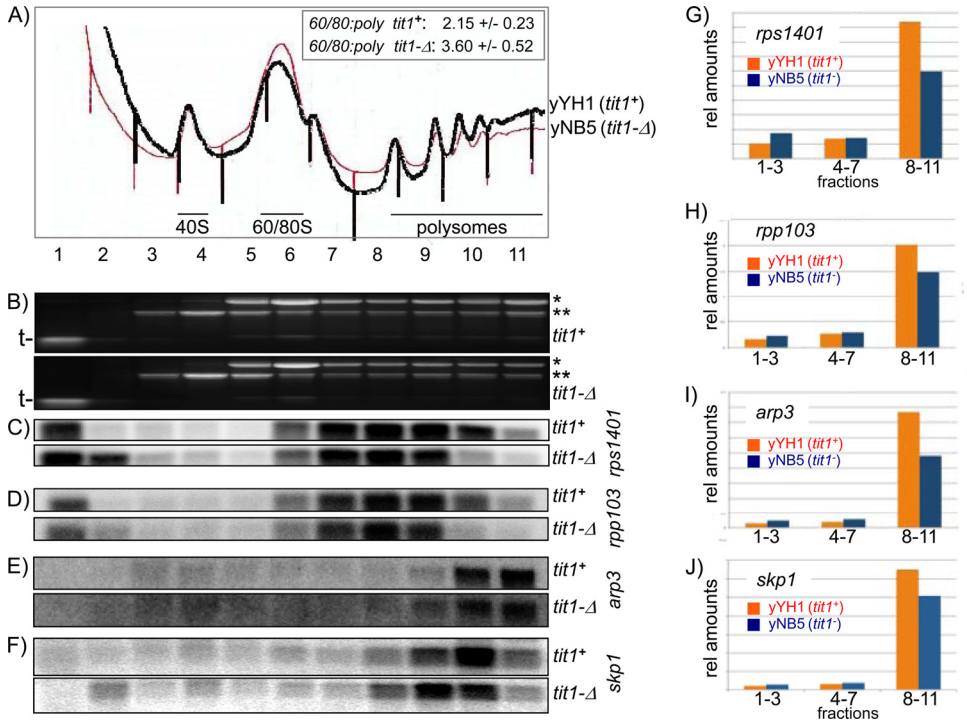

FIG 5 Deletion of *tit1* leads to decreased translation efficiency. (A) Sucrose gradient sedimentation polysome profiles of extracts from wild-type (black tracing; yYH1 *tit1*$^+$) and *tit1*-Δ (red tracing; yNB5) cells. Results of triplicate polysome profile quantitations are shown in the inset; the numbers report the means of three ratios of 60S plus 80S monosomes to polysomes. (B) Ethidium bromide-stained agarose gels of polysome fractions from yYH1 and yNB5 used for Northern blotting. Single and double asterisks to the right indicate 26S and 18S rRNAs, respectively, and "t-" to the left indicates the positions of the tRNAs. (C to F) Northern blots of RNAs isolated from the fractions in panel A, probed for *rps1401*, *rpp103*, *arp3*, and *skp1* mRNAs, respectively, as indicated to the right. (G to J) Quantification of the mRNAs in the blots shown in panels C to F. After quantification of individual bands, the relative amounts in the pooled fractions indicated on the *x* axis were plotted.

translated. We isolated RNAs from the polysome profile fractions shown in Fig. 5A (Fig. 5B). Northern blotting for *rps1401* (encoding 40S ribosomal protein S14) and *rpp103* (encoding 60S ribosomal protein L12P; also known as 60S acidic ribosomal protein P1) mRNAs revealed two notable differences in *tit1*$^+$ and *tit1*-Δ cells. First, there were more *rps1401* and *rpp103* mRNAs in the pre-40S fractions 2 and 3 of *tit1*-Δ cells than in those of *tit1*$^+$ cells, which is reflective of less efficient ribosome engagement. For both of these mRNAs, less than 9% of the total mRNA in all fractions was in the prepolysome fractions in *tit1*$^+$ cells, and this was increased to 27 to 35% in *tit1*-Δ cells (Fig. 5G and H). Second, *rps1401* (420 nucleotides [nt]; *Z* score = 4.1) and *rpp103* (330 nt; *Z* score = 3.7) mRNAs were found on larger polyribosomes in *tit1*$^+$ cells than in *tit1*-Δ cells (Fig. 5C and D). When these blots were probed for *arp3* mRNA (1,284 nt; *Z* score = 0.2), there was a less obvious difference in the profiles, likely because the *arp3* mRNA is longer, although quantitation clearly revealed a pattern of less efficient translation in *tit1*-Δ cells than in *tit1*$^+$ cells, similar to the patterns for *rps1401* and *rpp103* (Fig. 5E and I). The pattern obtained on the same blots for *skp1* mRNA (486 nt; *Z* score = −1.3) reflected a more efficient overall translation than that observed for *rps1401* and *rpp103*, although the difference between *tit1*-Δ and *tit1*$^+$ cells was smaller than those for the other mRNAs (Fig. 5F and J). These data are consistent with a complex pattern of altered translation in *tit1*-Δ cells, in part due to direct effects of decoding caused by lack of i6A37 and in part due to indirect effects related to a translational (and/or metabolic) stress response, as suggested by rapamycin sensitivity that is likely reflective of altered TOR signaling to the translation regulatory apparatus (see Discussion).

DISCUSSION

Here we report an analysis of tRNA-i6A37 function in fission yeast. While the most direct result of *tit1*$^+$ deletion is i6A37 hypomodification of Tit1 tRNA substrates (18), we demonstrated defects in codon-specific decoding by using a *lacZ* reporter. The presence of i6A37 on tRNA^{Cys}GCA increased its activity for the cognate codon. i6A37 increased the ability of tRNA^{Cys}GCA to protect its cognate codon against misreading by tRNA^{Tyr}GUA. Surprisingly, i6A37 also increased tRNA^{Tyr}GUA misreading of a near-cognate Cys codon. Thus, a unifying activity appears to be that i6A37 increases affinity of the tRNA for the ribosome decoding center, at least when the tRNA is occupied by a cognate or near-cognate codon. In terms of fidelity, it appears that i6A37 increases fidelity at cognate codons and decreases fidelity at noncognate codons.

tit1 mutant cells appear to sense and react to an altered state of translation, manifested by two phenotypes: sensitivity to rapamycin, which inhibits the TOR signaling pathway, and slow growth in glycerol. The TOR pathway senses and reacts to the metabolic and growth states of cells. As alluded to above, a relationship between altered translation, metabolic activity, and TOR signaling has become apparent in *S. pombe* (46). TOR signaling affects the phosphorylation of *S. pombe* ribosomal protein S6 (Rps6) (64). In ad-

dition, Psk1, which is necessary for Rps6 phosphorylation, is regulated by TORC1 in *S. pombe*, in nutrient-dependent and rapamycin-sensitive manners (65). In summary, the results of this report support others that indicate that disruptions in tRNA homeostasis or function, nutrient metabolism, or rapamycin itself induce compensatory signaling to the translational machinery in *S. pombe* (46, 65). Both the rapamycin and glycerol phenotypes are rescued by ectopic *tit1*$^+$ but not *tit1*-T12A, which is catalytically deficient for tRNA i6A transferase activity, providing evidence that they are due to a lack of tRNA modification. By computationally identifying the mRNAs most enriched in i6A37-cognate codons as those encoding ribosomal subunits and metabolic enzymes, the results help to explain the *S. pombe* phenotypes due to deletion of *tit1*$^+$.

Sucrose gradient sedimentation showed increased levels of 60S plus 80S monosomes relative to polysomes in *tit1*-Δ cells, consistent with the idea that translation was globally compromised (Fig. 5A). This is consistent with the fact that the family of ribosomal subunit mRNAs identified as overenriched in i6A37-cognate codons are each present at very high abundance and therefore collectively engage a significant fraction of the translation machinery. We provided evidence, in the form of mRNA distributions on polysome profiles, that translation of the highly abundant cellular mRNAs *rps1401* and *rpp103* (encoding ribosomal subunits), which are enriched with i6A37-cognate codons, is compromised in *tit1*-Δ cells.

The *skp1* and *arp3* mRNAs, which have less i6A37-cognate codon enrichment and lower abundances, also showed evidence of less translational efficiency in *tit1*-Δ cells, although to a slightly lesser degree than that for *rps1401* and *rpp103*. These analyses suggest that direct effects of i6A37 deficiency on cognate codon-enriched mRNAs are probably not the sole mechanism to account for the apparent translational compromise in *tit1*-Δ cells. We emphasize as an alternative that the effects of i6A37 deficiency may be due to both direct effects on translation efficiency and fidelity and indirect effects mediated by stress response signaling, in part through the TOR pathway, the sum of which is responsible for the observed phenotypes (66).

It is noteworthy that a 3-fold increase in tRNA^{Cys}GCA-G37 levels resulted in only an ~15% decrease in the tRNA^{Tyr}GUA-i6A37-mediated misreading in the *tit1*$^+$ cells (Fig. 2A). This disproportionately low level of decrease may reflect the fact that overexpression may have exhausted an activity critical to tRNA^{Cys}GCA function. We also note that the 3-fold-overexpressed tRNA^{Cys}-GCA-A37 was hypomodified with i6A37, while endogenous substrates were fully modified. Nonetheless, the 3-fold increase in i6A37-modified tRNA^{Cys}GCA-A37 led to 3-fold inhibition of tRNA^{Tyr}GUA-i6A37-mediated misreading. It should also be considered that the tRNA^{Cys}GCA-A37 was artificially altered at position 37 and that this might offset an otherwise unique feature of the tRNA that is important for its function (67). Future studies can address this by using the natural *S. cerevisiae* tRNA^{Cys}GCA-A37 and *lacZ*-Y503 in *S. cerevisiae MOD5* and *mod5*-Δ cells, as well as in *S. pombe tit1*$^+$ and *tit1*-Δ cells.

A role for Tit1 in mitochondrial function. Because slow growth on glycerol is common to mutants of mitochondrial function, it should be expected that this phenotype might be due, at least in part, to i6A37 hypomodification of mt-tRNA^{Trp}. However, hypomodification of cytoplasmic tRNAs involved in the translation of nucleus-encoded proteins that function in mitochondria might also contribute.

We used established computational programs to examine Tit1 and MOD5 sequences for predicted potential for mitochondrial targeting. According to the programs Predotar (68) and TargetP 1.1 (69), the fractions of total Tit1 and MOD5 proteins predicted for mitochondrial localization ranged from 18 to 36% for Tit1 and 23 to 47% for MOD5. Mito-prot-II (V1.101) (70) predicted the probability of export to mitochondria as 0.76 for Tit1 and 0.77 for MOD5. Thus, predictive programs and our results showing *tit1*$^+$-dependent i6A37 modification of mitochondrion-encoded mt-tRNA^{Trp} provide evidence that Tit1 is targeted to mitochondria.

Species-specific subsets of tRNAs that carry i6A37 also extend to mitochondria. Previous studies have shown that the subsets of tRNAs that carry i6A37 vary significantly, even among yeasts (18). Cytosolic tRNA^{Cys}GCA carries i6A37 in *S. cerevisiae* but not in *S. pombe*, whereas cytosolic tRNA^{Trp}CCA carries i6A37 in *S. pombe* but not in *S. cerevisiae* (18), and the distribution in human cells differs from those in both yeasts (Lamichhane and Maraia, unpublished data). We can now extend these disparities to mitochondrial tRNAs. mt-tRNA^{Cys} contains i6A37 in *S. cerevisiae* (19) but not in *S. pombe*, while mt-tRNA^{Trp} contains i6A37 in *S. pombe* but not in *S. cerevisiae*, and mt-tRNA^{Ser} contains i6A37 in human cells but not in either yeast species (T. Lamichhane, unpublished data).

In addition to species-specific disparities in i6A37-tRNAs, there are global differences in overall tRNA gene copy number and the fractional composition of isoacceptors (16). tRNA gene copy number can vary much more than most other features of highly related genomes of related species (16). Striking reformations of the relative numbers of isoacceptor tRNA genes within synonymous codon groups have occurred in highly related genomes (16). These variables likely affect the degree to which different tRNAs compete for cognate versus near-cognate codons and, therefore, misreading rates. This suggests that although the same genetic code is shared by a vast number of species, its translation occurs in somewhat of a species-specific manner, governed at least in part by the composition and modification characteristics of the tRNAome. Similarly, codon biases in mRNAs that encode otherwise homologous proteins may be subjected to species-specific translation due to differential codon use and tRNAome composition. These genome variables would differentially sensitize subsets of mRNAs to Tit1 homologs in different species. Considerations of both the substrate tRNA isoacceptors and their cognate codon-sensitive mRNAs may help us to understand the variable pleiotropic effects of Tit1 deficiency in different species, including *S. cerevisiae* and *S. pombe*, and extending to the *C. elegans* life span gene *GRO-1* and the human tumor suppressor, TRIT1.

ACKNOWLEDGMENTS

We thank Tom Dever for discussions and Marty Blum for media.

The Intramural Research Program of the Eunice Kennedy Shriver National Institute of Child Health and Human Development, NIH, supports work in the Maraia lab. Work in the Begley lab is supported by the National Institutes of Health (grant 1R01ES017010).

REFERENCES

1. **Phizicky EM, Hopper AK.** 2010. tRNA biology charges to the front. Genes Dev. **24:**1832–1860.
2. **Bjork GR.** 1995. Biosynthesis and function of modified nucleosides, p

165–206. *In* Söll D, RajBhandary UL (ed), tRNA: structure, biosynthesis, and function. ASM Press, Washington, DC.
3. **Yokoyama S, Nishimura S.** 1995. Modified nucleosides and codon recognition, p 207–223. *In* Söll D, RajBhandary UL (ed), tRNA: structure, biosynthesis, and function. ASM Press, Washington, DC.
4. **Agris PF.** 2008. Bringing order to translation: the contributions of transfer RNA anticodon-domain modifications. EMBO Rep. **9:**629–635.
5. **Agris PF, Vendeix FA, Graham WD.** 2007. tRNA's wobble decoding of the genome: 40 years of modification. J. Mol. Biol. **366:**1–13.
6. **Begley U, Dyavaiah M, Patil A, Rooney JP, Direnzo D, Young CM, Conklin DS, Zitomer RS, Begley TJ.** 2007. Trm9-catalyzed tRNA modifications link translation to the DNA damage response. Mol. Cell **28:**860–870.
7. **Bauer F, Matsuyama A, Candiracci J, Dieu M, Scheliga J, Wolf DA, Yoshida M, Hermand D.** 2012. Translational control of cell division by elongator. Cell Rep. **1:**424–433.
8. **Yarus M.** 1982. Translational efficiency of transfer RNA's: uses of an extended anticodon. Science **218:**646–652.
9. **Miyauchi K, Kimura S, Suzuki T.** 2013. A cyclic form of N6-threonylcarbamoyladenosine as a widely distributed tRNA hypermodification. Nat. Chem. Biol. **9:**105–111.
10. **Scott LJ, Mohlke KL, Bonnycastle LL, Willer CJ, Li Y, Duren WL, Erdos MR, Stringham HM, Chines PS, Jackson AU, Prokunina-Olsson L, Ding CJ, Swift AJ, Narisu N, Hu T, Pruim R, Xiao R, Li XY, Conneely KN, Riebow NL, Sprau AG, Tong M, White PP, Hetrick KN, Barnhart MW, Bark CW, Goldstein JL, Watkins L, Xiang F, Saramies J, Buchanan TA, Watanabe RM, Valle TT, Kinnunen L, Abecasis GR, Pugh EW, Doheny KF, Bergman RN, Tuomilehto J, Collins FS, Boehnke M.** 2007. A genome-wide association study of type 2 diabetes in Finns detects multiple susceptibility variants. Science **316:**1341–1345.
11. **Wei F, Suzuki T, Watanabe S, Kimura S, Kaitsuka T, Fujimura A, Matsui H, Atta M, Michiue H, Fontecave M, Yamagata K, Suzuki T, KT.** 2011. Deficit of tRNALys modification by Cdkal1 causes the development of type 2 diabetes in mice. J. Clin. Invest. **121:**3598–3608.
12. **Reynolds NM, Lazazzera BA, Ibba M.** 2010. Cellular mechanisms that control mistranslation. Nat. Rev. Microbiol. **8:**849–856.
13. **Kramer EB, Vallabhaneni H, Mayer LM, Farabaugh PJ.** 2010. A comprehensive analysis of translational missense errors in the yeast Saccharomyces cerevisiae. RNA **16:**1797–1808.
14. **Roy H, Ibba M.** 2006. Molecular biology: sticky end in protein synthesis. Nature **443:**41–42.
15. **Kramer EB, Farabaugh PJ.** 2007. The frequency of translational misreading errors in E. coli is largely determined by tRNA competition. RNA **13:**87–96.
16. **Iben JR, Maraia RJ.** 2012. Yeast tRNAomics: tRNA gene copy number variation and codon use provide bioinformatics evidence of a new wobble pair in a eukaryote. RNA **18:**1358–1372.
17. **Kwapisz M, Smagowicz WJ, Oficjalska D, Hatin I, Rousset JP, Zoladek T, Boguta M.** 2002. Up-regulation of tRNA biosynthesis affects translational readthrough in maf1-delta mutant of Saccharomyces cerevisiae. Curr. Genet. **42:**147–152.
18. **Lamichhane TN, Blewett NH, Maraia RJ.** 2011. Plasticity and diversity of tRNA anticodon determinants of substrate recognition by eukaryotic A37 isopentenyltransferases. RNA **17:**1846–1857.
19. **Dihanich ME, Najarian D, Clark R, Gillman EC, Martin NC, Hopper AK.** 1987. Isolation and characterization of MOD5, a gene required for isopentenylation of cytoplasmic and mitochondrial tRNAs of Saccharomyces cerevisiae. Mol. Cell. Biol. **7:**177–184.
20. **Lemieux J, Lakowski B, Webb A, Meng Y, Ubach A, Bussiere F, Barnes T, Hekimi S.** 2001. Regulation of physiological rates in Caenorhabditis elegans by a tRNA-modifying enzyme in the mitochondria. Genetics **159:**147–157.
21. **Soderberg T, Poulter CD.** 2000. Escherichia coli dimethylallyl diphosphate:tRNA dimethylallyltransferase: essential elements for recognition of tRNA substrates within the anticodon stem-loop. Biochemistry **39:**6546–6553.
22. **Spinola M, Galvan A, Pignatiello C, Conti B, Pastorino U, Nicander B, Paroni R, Dragani TA.** 2005. Identification and functional characterization of the candidate tumor suppressor gene TRIT1 in human lung cancer. Oncogene **24:**5502–5509.
23. **Spinola M, Colombo F, Falvella FS, Dragani TA.** 2007. N6-isopentenyladenosine: a potential therapeutic agent for a variety of epithelial cancers. Int. J. Cancer **120:**2744–2748.
24. **Persson BC, Esberg B, Olafsson O, Bjork GR.** 1994. Synthesis and function of isopentenyl adenosine derivatives in tRNA. Biochimie **76:**1152–1160.
25. **Laten H, Gorman J, Bock RM.** 1978. Isopentenyladenosine deficient tRNA from an antisuppressor mutant of Saccharomyces cerevisiae. Nucleic Acids Res. **5:**4329–4342.
26. **Gefter ML, Russell RL.** 1969. Role modifications in tyrosine transfer RNA: a modified base affecting ribosome binding. J. Mol. Biol. **39:**145–157.
27. **Diaz I, Pedersen S, Kurland CG.** 1987. Effects of miaA on translation and growth rates. Mol. Gen. Genet. **208:**373–376.
28. **Ericson JU, Bjork GR.** 1986. Pleiotropic effects induced by modification deficiency next to the anticodon of tRNA from Salmonella typhimurium LT2. J. Bacteriol. **166:**1013–1021.
29. **Esberg B, Bjork GR.** 1995. The methylthio group (ms2) of N6-(4-hydroxyisopentenyl)-2-methylthioadenosine (ms2io6A) present next to the anticodon contributes to the decoding efficiency of the tRNA. J. Bacteriol. **177:**1967–1975.
30. **Janner F, Vogeli G, Fluri R.** 1980. The antisuppressor strain sin1 of Schizosaccharomyces pombe lacks the modification isopentenyladenosine in transfer RNA. J. Mol. Biol. **139:**207–219.
31. **Kohli J, Munz P, Soll D.** 1989. Informational suppression, transfer RNA, and intergenic conversion, p 75–96. *In* Nasim A, Young P, Johnson BF (ed), Molecular biology of the fission yeast. Academic Press, Inc., San Diego, CA.
32. **Jenner LB, Demeshkina N, Yusupova G, Yusupov M.** 2010. Structural aspects of messenger RNA reading frame maintenance by the ribosome. Nat. Struct. Mol. Biol. **17:**555–560.
33. **Nielsen DA, Chou J, MacKrell AJ, Casadaban MJ, Steiner DF.** 1983. Expression of a preproinsulin-beta-galactosidase gene fusion in mammalian cells. Proc. Natl. Acad. Sci. U. S. A. **80:**5198–5202.
34. **Yang R, Gaidamakov SA, Xie J, Lee J, Martino L, Kozlov G, Crawford AK, Russo AN, Conte MR, Gehring K, Maraia RJ.** 2011. LARP4 binds poly(A), interacts with poly(A)-binding protein MLLE domain via a variant PAM2w motif and can promote mRNA stability. Mol. Cell. Biol. **31:**542–556.
35. **Carbon S, Ireland A, Mungall CJ, Shu S, Marshall B, Lewis S, AmiGO Hub, Web Presence Working Group.** 2009. AmiGO: online access to ontology and annotation data. Bioinformatics **25:**288–289.
36. **Diaz I, Ehrenberg M.** 1991. ms2i6A deficiency enhances proofreading in translation. J. Mol. Biol. **222:**1161–1171.
37. **Ring M, Bader DE, Huber RE.** 1988. Site-directed mutagenesis of beta-galactosidase (E. coli) reveals that tyr-503 is essential for activity. Biochem. Biophys. Res. Commun. **152:**1050–1055.
38. **Ring M, Huber RE.** 1990. Multiple replacements establish the importance of tyrosine-503 in beta-galactosidase (Escherichia coli). Arch. Biochem. Biophys. **283:**342–350.
39. **Penner RM, Roth NJ, Rob B, Lay H, Huber RE.** 1999. Tyr-503 of beta-galactosidase (Escherichia coli) plays an important role in degalactosylation. Biochem. Cell Biol. **77:**229–236.
40. **Hagervall TG, Pomerantz SC, McCloskey JA.** 1998. Reduced misreading of asparagine codons by Escherichia coli tRNALys with hypomodified derivatives of 5-methylaminomethyl-2-thiouridine in the wobble position. J. Mol. Biol. **284:**33–42.
41. **Chan PP, Lowe TM.** 2009. GtRNAdb: a database of transfer RNA genes detected in genomic sequence. Nucleic Acids Res. **37:**D93–D97.
42. **Johansson M, Zhang J, Ehrenberg M.** 2012. Genetic code translation displays a linear trade-off between efficiency and accuracy of tRNA selection. Proc. Natl. Acad. Sci. U. S. A. **109:**131–136.
43. **Weisman R, Choder M, Koltin Y.** 1997. Rapamycin specifically interferes with the developmental response of fission yeast to starvation. J. Bacteriol. **179:**6325–6334.
44. **Weisman R, Roitburg I, Nahari T, Kupiec M.** 2005. Regulation of leucine uptake by tor1+ in Schizosaccharomyces pombe is sensitive to rapamycin. Genetics **169:**539–550.
45. **Takahara T, Maeda T.** 2012. TORC1 of fission yeast is rapamycin-sensitive. Genes Cells **17:**698–708.
46. **Cherkasova V, Bahler J, Bacikova D, Pridham K, Maraia RJ.** 2012. Altered nuclear tRNA metabolism in La-deleted *Schizosaccharomyces pombe* is accompanied by a nutritional stress response involving Atf1p and Pcr1p that is suppressible by Xpo-t/Los1p. Mol. Biol. Cell **23:**480–491.
47. **Nurse P.** 2004. Wee beasties. Nature **432:**557.

48. **Nurse P, Thuriaux P.** 1980. Regulatory genes controlling mitosis in the fission yeast Schizosaccharomyces pombe. Genetics **96:**627–637.
49. **Yanagida M, Ikai N, Shimanuki M, Sajiki K.** 2011. Nutrient limitations alter cell division control and chromosome segregation through growth-related kinases and phosphatases. Philos. Trans. R. Soc. Lond. B Biol. Sci. **366:**3508–3520.
50. **Kellogg DR.** 2003. Wee1-dependent mechanisms required for coordination of cell growth and cell division. J. Cell Sci. **116:**4883–4890.
51. **Saracino F, Bassler J, Muzzini D, Hurt E, Agostoni Carbone ML.** 2004. The yeast kinase Swe1 is required for proper entry into cell cycle after arrest due to ribosome biogenesis and protein synthesis defects. Cell Cycle **3:**648–654.
52. **Vassarotti A, Boutry M, Colson AM, Goffeau A.** 1984. Independent loci for the structural genes of the yeast mitochondrial alpha and beta ATPase subunits. J. Biol. Chem. **259:**2845–2849.
53. **Gillman EC, Slusher LB, Martin NC, Hopper AK.** 1991. MOD5 translation initiation sites determine N6-isopentenyladenosine modification of mitochondrial and cytoplasmic tRNA. Mol. Cell. Biol. **11:**2382–2390.
54. **Murawski M, Szczesniak B, Zoladek T, Hopper AK, Martin NC, Boguta M.** 1994. maf1 mutation alters the subcellular localization of the Mod5 protein in yeast. Acta Biochim. Pol. **41:**441–448.
55. **Tolerico LH, Benko AL, Aris JP, Stanford DR, Martin NC, Hopper AK.** 1999. Saccharomyces cerevisiae Mod5p-II contains sequences antagonistic for nuclear and cytosolic locations. Genetics **151:**57–75.
56. **Zoladek T, Vaduva G, Hunter LA, Boguta M, Go BD, Martin NC, Hopper AK.** 1995. Mutations altering the mitochondrial-cytoplasmic distribution of Mod5p implicate the actin cytoskeleton and mRNA 3′ ends and/or protein synthesis in mitochondrial delivery. Mol. Cell. Biol. **15:**6884–6894.
57. **Motorin Y, Bec G, Tewari R, Grosjean H.** 1997. Transfer RNA recognition by the Escherichia coli delta2-isopentenyl-pyrophosphate:tRNA delta2-isopentenyl transferase: dependence on the anticodon arm structure. RNA **3:**721–733.
58. **Bennetzen JL, Hall BD.** 1982. Codon selection in yeast. J. Biol. Chem. **257:**3026–3031.
59. **Fuchs BB, Mylonakis E.** 2009. Our paths might cross: the role of the fungal cell wall integrity pathway in stress response and cross talk with other stress response pathways. Eukaryot. Cell **8:**1616–1625.
60. **Marguerat S, Schmidt A, Codlin S, Chen W, Aebersold R, Bahler J.** 2012. Quantitative analysis of fission yeast transcriptomes and proteomes in proliferating and quiescent cells. Cell **151:**671–683.
61. **Bouadloun F, Srichaiyo T, Isaksson LA, Bjork GR.** 1986. Influence of modification next to the anticodon in tRNA on codon context sensitivity of translational suppression and accuracy. J. Bacteriol. **166:**1022–1027.
62. **Hartwell LH, McLaughlin CS.** 1969. A mutant of yeast apparently defective in the initiation of protein synthesis. Proc. Natl. Acad. Sci. U. S. A. **62:**468–474.
63. **Foiani M, Cigan AM, Paddon CJ, Harashima S, Hinnebusch AG.** 1991. GCD2, a translational repressor of the GCN4 gene, has a general function in the initiation of protein synthesis in Saccharomyces cerevisiae. Mol. Cell. Biol. **11:**3203–3216.
64. **Nakashima A, Sato T, Tamanoi F.** 2010. Fission yeast TORC1 regulates phosphorylation of ribosomal S6 proteins in response to nutrients and its activity is inhibited by rapamycin. J. Cell Sci. **123:**777–786.
65. **Nakashima A, Otsubo Y, Yamashita A, Sato T, Yamamoto M, Tamanoi F.** 2012. Psk1, an AGC kinase family member in fission yeast, is directly phosphorylated and controlled by TORC1 and functions as S6 kinase. J. Cell Sci. **125:**5840–5849.
66. **Chan CT, Pang YL, Deng W, Babu IR, Dyavaiah M, Begley TJ, Dedon PC.** 2012. Reprogramming of tRNA modifications controls the oxidative stress response by codon-biased translation of proteins. Nat. Commun. **3:**937.
67. **Olejniczak M, Dale T, Fahlman RP, Uhlenbeck OC.** 2005. Idiosyncratic tuning of tRNAs to achieve uniform ribosome binding. Nat. Struct. Mol. Biol. **12:**788–793.
68. **Small I, Peeters N, Legeai F, Lurin C.** 2004. Predotar: a tool for rapidly screening proteomes for N-terminal targeting sequences. Proteomics **4:**1581–1590.
69. **Emanuelsson O, Brunak S, von Heijne G, Nielsen H.** 2007. Locating proteins in the cell using TargetP, SignalP and related tools. Nat. Protoc. **2:**953–971.
70. **Claros MG.** 1995. MitoProt, a Macintosh application for studying mitochondrial proteins. Comput. Appl. Biosci. **11:**441–447.
71. **Huang Y, Intine RV, Mozlin A, Hasson S, Maraia RJ.** 2005. Mutations in the RNA polymerase III subunit Rpc11p that decrease RNA 3′ cleavage activity increase 3′-terminal oligo(U) length and La-dependent tRNA processing. Mol. Cell. Biol. **25:**621–636.
72. **Intine RVA, Sakulich AL, Koduru SB, Huang Y, Pierstorrf E, Goodier JL, Phan L, Maraia RJ.** 2000. Control of transfer RNA maturation by phosphorylation of the human La antigen on serine 366. Mol. Cell **6:**339–348.